Science of the Total Environment 794 (2021) 148757

Contents lists available at ScienceDirect

Science of the Total Environment

journal homepage: www.elsevier.com/locate/scitotenv

Biochar-based fertilizer amendments improve the soil microbial community structure in a karst mountainous area

Taotao Yan [a,b], Jianhui Xue [a,b,c,*], Zhidong Zhou [b,c], Yongbo Wu [a,b]

[a] College of Biology and the Environment, Nanjing Forestry University, Nanjing, China
[b] Co-Innovation Center for Sustainable Forestry in Southern China, Nanjing Forestry University, Nanjing, China
[c] Institute of Botany, Jiangsu Province and Chinese Academy of Sciences, Nanjing, China

HIGHLIGHTS

- Biochar-based fertilization altered the nutrient status and microbial community structure of karst soils.
- Biochar-based fertilizer amendment resulted in the activation of more OTUs and more complex interspecific interactions.
- Biochar-based fertilizer enabled more keystone species to participate in carbon resource management and nutrient cycling.

GRAPHICAL ABSTRACT

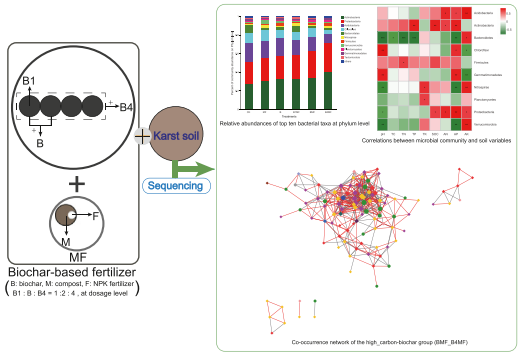

ARTICLE INFO

Article history:
Received 7 December 2020
Received in revised form 29 April 2021
Accepted 26 June 2021
Available online 29 June 2021

Editor: Baoliang Chen

Keywords:
Karst soil
Biochar-based fertilizer
Soil properties
Microbial community structure
Microbial network

ABSTRACT

Biochar-based fertilizer amendment can improve soil properties partly due to stimulated microbial activities and growths. The karst ecosystem is prone to degradation and accounts for a large proportion of southwest China. Understanding of the response of the microbial community structure to biochar-based fertilizer application is of great significance in karst soil restoration. A field experiment located in southwest China was conducted in typical karst soil, and a high-throughput sequencing approach was used to investigate the effect of biochar-based fertilizer application on microbial community structure in karst soil. Field trials were set up for 24 months using the following treatments: control (CK), compost plus NPK fertilizer (MF), biochar (B), less biochar (half the quantity of biochar in B) plus compost and NPK fertilizer (B1MF), biochar plus compost and NPK fertilizer (BMF), and more biochar (double the quantity of biochar in B) plus compost and NPK fertilizer (B4MF). The results elucidated that BMF and B4MF treatments had higher contents of soil carbon and soil nutrients N, P, and K than the other treatments. Soil microbial abundance and diversity were significantly increased by biochar-based fertilizer amendments (BMF and B4MF), compared to CK ($P < 0.05$). BMF and B4MF treatments significantly increased the relative abundance of dominant microorganisms, compared to CK ($P < 0.05$). The difference in the composition of indicator microbes between each treated group indicated that soil amendments altered the microbial community structure. There was a strong correlation between soil properties (soil C-, N-, and P-fractions) and microbial community structure. Furthermore, network analysis revealed that the addition of biochar-based fertilizer increased the scale and complexity of the microbial co-occurrence network. To summarize, the application of biochar-based fertilizer enabled more keystone species in the soil microbial network to participate in soil carbon resource management and soil nutrient cycling, indicating that biochar-based fertilizer is beneficial for the restoration of karst-degraded soils.

* Corresponding author at: College of Biology and the Environment, Nanjing Forestry University, Nanjing, China.
E-mail addresses: ecologyan@njfu.edu.cn (T. Yan), jhxue@njfu.edu.cn (J. Xue).

https://doi.org/10.1016/j.scitotenv.2021.148757
0048-9697/

1. Introduction

The karst landform is a geological landscape with special hydrological conditions and geomorphological features. It is formed under certain geological, climatic, and hydrological conditions by the erosion and transformation of soluble rocks (mainly carbonate rocks) mediated by surface water and groundwater, which is produced by the combination of highly soluble rocks and fully developed secondary pores (Ford and Williams, 2007). The distribution area of karst landforms accounts for approximately 12.53% of the global land area (except Antarctica, Greenland and Iceland), and southwestern China is the largest concentrated and contiguous karst region in the world (Ford and Williams, 2007; Liu et al., 2016). Karst ecosystems are extremely vulnerable and prone to rocky desertification (Liang et al., 2015). Rocky desertification is the land degradative process during which human activities interfere with surface vegetation and cause severe soil erosion, large bedrock exposure, severe degradation of land productivity, and desert-like landscape under the natural background of humid and semi-humid climate conditions and karst development in tropical and subtropical regions (Williams, 1993; Sauro, 1993; Yuan, 1997). Karst rocky desertification leads to significant negative impacts on the local natural environment and socio-economic conditions (Chen et al., 2011; Jiang et al., 2014). Ecological restoration measures such as afforestation and soil improvement have been applied to combat karst rocky desertification (Li et al., 2020a, 2020b). In agricultural soil, biochar has proven to be a promising soil amendment (Yao et al., 2017). Thus, in the present study, we applied biochar to karst soil with the expectation that it would have a positive and beneficial impact on the soil nutrient status and microbial community structure of karst soil.

As a carbon-rich material, biochar is produced from biomass raw materials such as crop residues or wood under anoxic conditions at a pyrolysis temperature of <700 °C (Marris, 2006; Roberts et al., 2010). Biochar has a stable structure and is not easily decomposed by microbes (Chun et al., 2004; Gaunt and Lehmann, 2008). It is a porous alkaline material with strong adsorption ability, huge surface area, and low bulk density (Atkinson et al., 2010; Dumroese et al., 2011). Biochar addition changes the physical properties of soil, increasing porosity and decreasing soil bulk density, which facilitates aggregate formation, thereby improving the soil structure (Fungo et al., 2017; Pituello et al., 2018). Biochar can alter the chemical properties of soil by enlarging cation exchange capacity (CEC) (Chintala et al., 2014). It also increases the pH of acidic soils (Van Zwieten et al., 2010), and can quickly enhance the organic carbon contents of soil (Liu et al., 2012). Biochar can be used as an absorbent to increase nitrogen use efficiency and reduce nitrogen leaching (Xu et al., 2016). The surface area and porosity of biochar are crucial for soil nutrient maintenance because both cations and anions are bound to its surface (Liang et al., 2008; Chan and Xu, 2009; Ding et al., 2010; Xu et al., 2014). The strong adsorption of NH_4^+ on biochar can reduce nitrogen volatilization (Bai et al., 2015), thereby improving soil fertility and stimulating plant growth and development (Alburquerque et al., 2014; Macdonald et al., 2014). Biochar can modulate microbial community structure and enzyme activity in soil by increasing the microbial respiration rate (Steiner et al., 2007; Lehmann et al., 2011; Rex et al., 2015). This can be done by enhancing microbial biomass nitrogen, carbon, and phosphorus (Kuzyakov et al., 2009; Zhang et al., 2015; Manirakiza et al., 2019) and by stimulating soil bacterial growth, especially diazotrophs (Deluca et al., 2009; Liu et al., 2019). Biochar addition can reduce soil heterotrophic respiration through increasing soil organic carbon recalcitrancy and decreasing activities of carbon-degrading enzymes (Li et al., 2018). Furthermore, biochar can offer a physical niche for hyphae growth without fungal herbivores, thereby stimulating the growth of soil fungi (Hammer et al., 2014). Considering the pore size of biochar, soil herbivores larger than collembola and smaller than protozoans are excluded (Atkinson et al., 2010). For example, the root colonization sites of several arbuscular mycorrhizae are increased with biochar (Warnock et al., 2007; Atkinson et al., 2010). Additionally, biochar possesses a potential synergistic effect on increasing the abundance and activity of mycorrhizal fungi and promoting their penetration in plant roots for colonization (Warnock et al., 2010; Yin et al., 2016). The fine-structured biochar pores can reduce the oxygen concentration by making the oxygen be dissolved in pore water and allowing the oxygen to occupy the air-filled pore space, thereby ensuring nitrogenase activities (Thies and Rillig, 2009). However, previous research has demonstrated that the addition of biochar or biochar-based fertilizers significantly modulated the structure of the microbial community in soil, which varied depending on the methods of biochar application (e.g., applied alone or in combination with fertilizers) (Wu et al., 2016).

Soil microorganisms are closely connected with the soil physicochemical properties, including the formation of humus, soil organic matter decomposition, the transformation of soil substances, and nutrient cycling (Fierer, 2017). Additionally, due to the sensitivity of soil microorganisms to environmental changes, the community structure, composition, and diversity of soil microorganisms can be employed as crucial indicators for soil quality and fertility evaluation (Jeffries et al., 2003; Luo et al., 2016; Tian et al., 2018). Previous research revealed that land use intensity, as an important causal factor of karst ecosystem degradation, could alter the bacterial community structure and bacterial interactions in karst soils (Xue et al., 2020). The application of biochar in combination with chemical fertilizers could change the microbial community structure, enhance the microbial metabolic activity, and improve soil quality (Tian et al., 2016). Therefore, we hypothesized that understanding the response of microbial communities to biochar or biochar-based fertilizer could enable more effective amelioration of karst-degraded soils. Recently, high-throughput sequencing technology has become a powerful tool for studying soil microorganisms due to its advantages of high throughput, high accuracy, and ability to analyze a large number of samples simultaneously (Xia and Jia, 2014). Ecological network analysis is a method based on the random matrix theory (RMT) to study the internal interactions of ecosystems (Luo et al., 2007). With the development of this method, combined with data from high-throughput sequencing, a solution is provided for understanding the potential interactions within microbial communities (Zhou et al., 2010; Zhou et al., 2011).

This study aims to assess the potential improvements of biochar and biochar-based fertilizer on the soil nutrient status and soil microbial community structure of a karst mountainous area in southwestern China. We hypothesized that the application of biochar-based fertilizer in barren karst soil would i) change the soil microbial diversity, abundance and composition; ii) improve soil nutrient status because of biochar's ability to hold soil nutrients; and iii) increase the complexity of the soil microbial community network. Therefore, we performed a field experiment to evaluate the response of soil properties, soil microbial communities, and molecular ecological networks to biochar and biochar-based fertilizer.

2. Materials and methods

2.1. Experimental sites and biochar-based fertilizer

The study field was located in Puding County, Guizhou Province, China (105°45′33″E, 26°19′51″N). The study area is 1250 m above sea level. The typical karst landform in this area belongs to the humid north subtropical monsoon climate, with terrain slopes between 18 and 22 degrees, annual precipitation of 1396.9 mm, and an average annual temperature of 15.1 °C (Wang et al., 2014; Zhou et al., 2019). According to the Soil Survey Staff, the field soil is classified as sandy loam calcareous soil (Rendolls) (Soil Survey Staff, 2014). The resource and use of biochar-based fertilizer were according to our previous experimental method (Zhou et al., 2019). More details can be found in the supplementary files.

2.2. Experimental design and sample collection

As an important method of vegetation restoration, the black locust plantation is widely used to prevent rocky desertification in the karst area of southwestern China. We selected a black locust plantation established in 2014 for this study. Each treatment had 10 m × 10 m triplicate plots based on a randomized block design. There was a total of six treatments, including the control (CK), compost plus NPK fertilizer (MF), biochar (B), less biochar (half the quantity of biochar in B) plus compost and NPK fertilizer (B1MF), biochar plus compost and NPK fertilizer (BMF), and more biochar (double the quantity of biochar in B) plus compost and NPK fertilizer (B4MF). Biochar-based fertilizers (B1MF, BMF, and B4MF) were prepared following the method used in our previous study (Zhou et al., 2019). More details regarding the settings for each treatment are displayed in supplementary files and Table S1. Considering the thickness heterogeneity of karst soils, the surface soil at a depth of 10 cm in each plot was first mixed thoroughly with soil amendments using a shovel, and then the mixed soil was backfilled, evenly covered and lightly compacted. Considering the potential disturbance of the aforementioned process on surface plants, the same tillage was applied to CK.

The experiment was initiated on September 28, 2016, and the soil samples were collected after 24 months (October 2, 2018). Five soil samples were randomly collected using a soil corer (diameter: 50 mm) at a depth of 0–10 cm in each plot. These five soil samples were mixed to make a sample for each treatment. A total of 18 samples were collected, immediately placed in an icebox, and then transported to the laboratory for passing through a 2.0-mm sieve. Subsequently, one part of the sample was stored at 4 °C for analyzing soil chemical and physical properties, and the other part was stored at −80 °C for microbial sequencing.

2.3. Chemical analysis of the soil samples

The soil pH was measured at a soil:water ratio of 1:2.5 (w/v) using a pH meter (Metro-pH 320; Mettler-Toledo Instruments Ltd., Shanghai, China). The total nitrogen (TN) and total carbon (TC) were determined using a 2400 Series II CHNS/O System elemental analyzer (PerkinElmer Instruments Ltd., Shanghai, China). After reflux digestion with hydrofluoric acid nitric acid, and perchloric acid, the profile DV (Teledyne Leeman Labs, USA) inductively coupled plasma atomic emission spectrometer (ICP-AES) was employed to determine total Potassium (TK) and total phosphorus (TP). Soil organic carbon (SOC) was measured by the potassium dichromate oxidation-external heating method (Fan et al., 2017). Soil available nitrogen (AN) was measured by the alkali solution diffusion method (Webster, 2008). Soil available phosphorous (AP) was extracted with 0.5 M $NaHCO_3$ and determined by the molybdenum-antimony colorimetric method (Olsen, 1954). Available potassium (AK) was extracted with 1 M NH_4OAc and measured with a ScienNovo LT-FP6450 flame photometer (Shanghai Lilang Scientific Instrument Co., Ltd., Shanghai, China) (Lu, 1999).

2.4. Microbial high-throughput sequencing

Bacterial 16S ribosomal RNA (rRNA) genes were amplified by primers 338F (5′-ACTCCTACGGGAGGCAGCAG-3′) and 806R (5′-GGAC TACHVGGGTWTCTAAT-3′). Fungal internal transcribed spacer (ITS) rRNA genes were amplified by primers ITS1F (5′-CTTGGTCATTTAGA GGAAGTAA-3′) and ITS2R (5′-GCTGCGTTCTTCATCGATGC-3′). Sequencing was performed, based on an Illumina MiSeq platform (San Diego, CA, USA), by Shanghai Majorbio Bio-pharm Biotechnology Co., Ltd. (Shanghai, China). More details on the DNA metabarcoding molecular analyses can be found in the supplementary files. The 16S rRNA and ITS rRNA sequences were aligned with reference sequences based on the Silva database (http://www.arb-silva.de, version 132) (Quast et al., 2013) and Unite database (http://unite.ut.ee/index.php, version 8.0) (Kõljalg et al., 2005), respectively. The raw sequencing data have been uploaded to the NCBI Sequence Read Archive database (Bacterial Accession Number: SRP292159; Fungal Accession Number: SRP295589).

2.5. Statistical analysis

The calculation of microbial α-diversity was conducted using Mothur (version v.1.30.1) (Guo et al., 2019). The one-way analysis of variance (ANOVA) with Duncan's test was performed using SPSS software (version 19.0, Chicago, Illinois, USA) to analyze the differences in soil properties and soil microbial α-diversity. The analysis of microbial community composition, Principal coordinate analysis (PCoA), sample hierarchical clustering, linear discriminant analysis effect size (Lefse), redundancy analysis (RDA), and correlations of microbial community with soil variables were performed using the free online Majorbio Cloud Platform (https://cloud.majorbio.com/) (Ao et al., 2020).

2.6. Network analysis

According to previous descriptions (Shade and Handelsman, 2012; Wei et al., 2020), we selected the representative operational taxonomic units (OTUs) for network analysis. Additionally, according to the cluster analysis, we divided the samples into three groups for network analysis, namely, CK_MF, B_B1MF, and BMF_B4MF (classifying each pair as one treatment group). Three molecular ecological networks were constructed, namely, a CK- and MF-treated soil microbial network (the no-biochar network), a B- and B1MF-treated soil microbial network (the low_carbon-biochar network), and a BMF- and B4MF-treated soil microbial network (the high_carbon-biochar network). Using the high-throughput sequencing data from these three networks, the phylogenetic molecular ecology networks were constructed according to the RMT. Network construction and determination of network attribute parameters was performed on the Molecular Ecological Network Analysis Pipeline (MENA, http://ieg4.rccc.ou.edu/mena) (Zhou et al., 2010; Zhou et al., 2011; Deng et al., 2012). The major steps were as follows: the OTU data were classified and uploaded according to the MENA format. The correlation matrix was constructed by calculating the Pearson's correlation of any two OTUs (Horvath and Dong, 2008) and then the correlation matrix was converted into a similarity matrix. Based on the RMT, the similarity threshold was automatically identified, and then the similarity matrix was converted into an adjacency matrix to the connection strength between OTU nodes. According to the determined similarity threshold, the network properties were calculated (Network reports in MENA), and then by putting the network file and the node attribute file, Cytoscape 3.4.0 software was used to visualize the network (Shannon et al., 2003). Through network visualization, the network structure properties were displayed, including the number of nodes (i.e. the number of species in a network), the connection between nodes (i.e. the relationships between species), and the properties of modules (i.e. the characteristics of functional units in an ecosystem) (Newman, 2006; Zhou et al., 2010). Finally, the role of nodes was classified based on the connectivity among modules (Pi) and connectivity within modules (Zi), as well as the high mean node degree (Deng et al., 2012; Berry and Widder, 2014; Banerjee et al., 2019; Wei et al., 2020).

3. Results

3.1. Soil properties

The pH, TC, TK, SOC, AN and AP were significantly increased by soil amendments ($P < 0.05$). The soil C-, N-, and P-fractions (i.e. TC, TP, and AN) were significantly increased at B compared to MF (Table 1). The TN and TP were significantly increased by the biochar treatments (B, B1MF, BMF and B4MF, $P < 0.05$). The AK was significantly increased by MF, BMF, and B4MF treatments ($P < 0.05$). Additionally, all the soil

Table 1
Soil physicochemical properties under different treatments.

Treatments	pH	TC(%)	TN(%)	TP(g/kg)	TK(g/kg)	SOC(%)	AN(mg/kg)	AP(mg/kg)	AK(mg/kg)
CK	7.42 ± 0.05a	4.53 ± 0.08a	0.53 ± 0.03a	0.79 ± 0.24a	7.18 ± 0.10a	3.03 ± 0.07a	197.71 ± 6.64a	5.21 ± 0.20a	118.73 ± 1.44a
MF	7.51 ± 0.02b	6.00 ± 0.14b	0.69 ± 0.04ab	0.92 ± 0.37a	8.25 ± 0.10b	5.16 ± 0.11b	356.92 ± 23.49b	7.05 ± 0.14b	245.53 ± 55.46b
B	7.56 ± 0.08b	7.77 ± 0.12c	0.86 ± 0.06b	1.42 ± 0.07b	7.89 ± 0.08c	5.14 ± 0.03b	466.31 ± 3.03c	6.48 ± 0.57c	134.82 ± 8.50a
B1MF	7.53 ± 0.04b	8.53 ± 0.39d	0.96 ± 0.07bc	1.39 ± 0.12b	7.74 ± 0.13c	5.21 ± 0.08b	446.05 ± 8.74c	7.07 ± 0.08b	189.1 ± 17.29ab
BMF	7.65 ± 0.06c	10.81 ± 0.54e	1.07 ± 0.04c	1.85 ± 0.11c	10.27 ± 0.09d	6.23 ± 0.03c	560.80 ± 6.73d	7.95 ± 0.84d	332.08 ± 24.63c
B4MF	7.78 ± 0.07d	12.62 ± 0.29f	1.29 ± 0.05d	2.16 ± 0.22d	13.54 ± 0.09e	6.52 ± 0.06c	579.48 ± 10.92d	8.14 ± 0.63d	350.22 ± 9.54c
F values									
Treatments	28.51**	229.84**	56.76**	12.61**	69.38**	25.03**	63.77**	18.66**	30.9**

TC, total carbon; TN, total nitrogen; TP, total phosphorus; TK, total potassium; SOC, soil organic carbon; AN, available nitrogen; AP, available phosphorus; and AK, available potassium. The results were given as mean ± SD (standard deviation). Different lowercase letters within a column indicate significant differences at the $P = 0.05$ level among the different treatments.
** Statistically significant at $P = 0.01$, with Duncan's test.

properties were significantly increased by BMF and B4MF treatments ($P < 0.05$, Table 1). The B4MF treatment had the highest values of soil variables, but the differences of SOC, AN, AP, and AK between B4MF and BMF treatments were not significant ($P > 0.05$, Table 1). The one-way ANOVA indicated that the soil physicochemical properties were significantly affected by different treatments ($P < 0.01$) (Table 1).

3.2. Microbial α-diversity

OTUs (OTU quantities), diversity indices (Shannon and Simpson), and richness indices (ACE and Chao1) were compared between different treatments in bacterial and fungal communities, respectively (Table 2). Bacterial OTUs, Shannon diversity index, ACE richness index, and Chao1 richness index were significantly increased by soil amendments compared to CK ($P < 0.05$). Bacterial Simpson diversity was significantly increased by soil amendments compared to CK ($P < 0.05$). BMF and B4MF treatments had significantly higher bacterial OTU quantities than other treatments ($P < 0.05$). The bacterial Shannon diversity index significantly increased at BMF and B4MF treatments compared to CK, MF, and B treatments ($P < 0.05$). Except for comparison with CK, the bacterial Simpson diversity index did not change significantly between other treatments. ($P > 0.05$). B1MF, BMF and B4MF treatments had significantly higher bacterial ACE and Chao1 richness indices than other treatments ($P < 0.05$). The one-way ANOVA indicated that the treatments significantly affected the values of bacterial OTUs, Shannon diversity index, ACE richness index, Chao1 richness index ($P < 0.01$), and Simpson diversity index ($P < 0.05$, Table 2).

BMF and B4MF treatments significantly increased fungal OTU quantities (OTUs) and richness indices (ACE and Chao1) compared to CK ($P < 0.05$, Table 2). The fungal Shannon diversity index was significantly increased by soil amendments compared to CK ($P < 0.05$, Table 2). Fungal Simpson diversity significantly increased at BMF and B4MF treatments compared to CK, MF, and B treatments ($P < 0.05$, Table 2). The one-way ANOVA indicated that treatments significantly affected the values of fungal OTU quantities (OTUs) ($P < 0.05$) and diversity indices (Shannon and Simpson) ($P < 0.01$, Table 2).

3.3. Microbial community composition and structure

The relative abundances at the bacterial phylum level revealed that *Actinobacteria* was the most dominant phylum, followed by *Proteobacteria* (Fig. 1a). The relative abundances of *Actinobacteria* and *Proteobacteria* significantly increased at BMF (39.59% and 29.01%, respectively) and B4MF (41.14% and 30.37%, respectively) compared to CK (28.44% and 22.64%, respectively) ($P < 0.05$; Figs. 1a; S1a). On the phylum level of fungi, the values of relative abundances indicated that *Ascomycota* was the most dominant phylum, followed by *Mortierellomycota* (Fig. 1b). The relative abundances of *Ascomycota* were significantly increased by soil amendments compared to CK ($P < 0.05$; Figs. 1b; S1b). BMF (79.65%) and B4MF (84.38%) treatments had significantly higher relative abundances of *Ascomycota* than other treatments ($P < 0.05$; Figs. 1b; S1b). Except for the MF treatment, soil amendments significantly increased the relative abundances of *Mortierellomycota* compared to CK ($P < 0.05$; Figs. 1b; S1b). The BMF treatment (15.5%) had the highest relative abundance of *Mortierellomycota* compared to other treatments ($P < 0.05$; Figs. 1b; S1b).

The PCoA on the OTU level clearly distinguished among the soil bacterial and fungal communities under different treatments, respectively

Table 2
Estimated numbers of observed richness and diversity for different treatments.

Treatments	OTUs	Shannon	Simpson	ACE	Chao1
Bacteria					
CK	1771.33 ± 50.33a	6.18 ± 0.08a	0.0061 ± 0.0009a	2199.11 ± 83.77a	2202.71 ± 44.55a
MF	1869.00 ± 49.87b	6.34 ± 0.06b	0.0040 ± 0.0006b	2356.18 ± 28.19b	2375.89 ± 54.45b
B	1874.33 ± 13.87b	6.37 ± 0.08bc	0.0040 ± 0.0005b	2420.65 ± 12.32b	2401.70 ± 25.61b
B1MF	1990.67 ± 26.95c	6.47 ± 0.06 cd	0.0041 ± 0.0004b	2536.48 ± 20.81c	2544.74 ± 31.69c
BMF	2073.00 ± 38.22d	6.51 ± 0.05d	0.0039 ± 0.0005b	2577.00 ± 32.67c	2596.66 ± 57.03c
B4MF	2095.33 ± 36.12d	6.58 ± 0.05d	0.0037 ± 0.0004b	2588.96 ± 36.36c	2575.93 ± 38.09c
F values					
Treatments	33.91**	9.73**	7.48*	38.53**	36.69**
Fungi					
CK	526.33 ± 172.24a	3.66 ± 0.14a	0.0823 ± 0.0147a	578.06 ± 216.44a	579.30 ± 215.04a
MF	620.00 ± 74.75ab	3.89 ± 0.15b	0.0723 ± 0.0116ab	774.30 ± 35.97ab	771.80 ± 34.89ab
B	673.67 ± 10.50ab	3.89 ± 0.07b	0.0667 ± 0.0112ab	814.38 ± 62.49ab	817.04 ± 67.53ab
B1MF	678.00 ± 73.51ab	3.91 ± 0.10b	0.0569 ± 0.0085bc	711.95 ± 128.62ab	709.41 ± 119.73ab
BMF	755.00 ± 37.00b	4.26 ± 0.15c	0.0408 ± 0.0116 cd	836.00 ± 128.35b	835.80 ± 125.15b
B4MF	791.33 ± 78.04b	4.40 ± 0.05c	0.0363 ± 0.0054d	890.47 ± 104.68b	883.58 ± 108.47b
F values					
Treatments	3.36*	16.96**	8.26**	2.29	2.28

The results were given as mean ± SD (standard deviation). Different lowercase letters within a column indicate significant differences at the $P = 0.05$ level among the different treatments.
* and ** are statistically significant at $P = 0.05$ and $P = 0.01$ with Duncan's test, respectively.

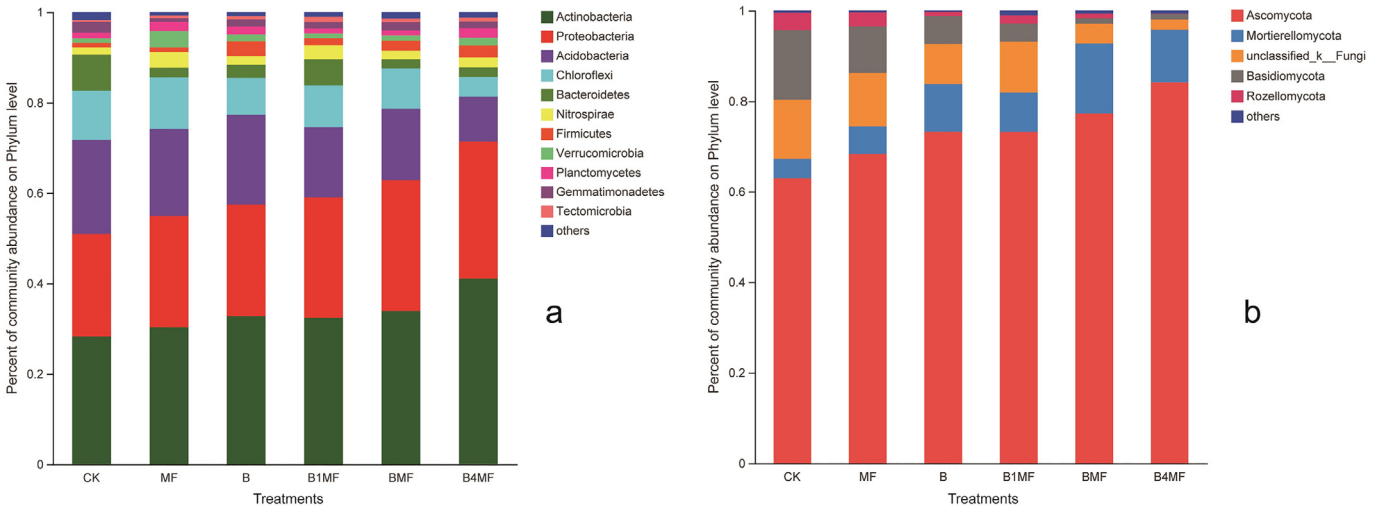

Fig. 1. Relative abundances on phylum level of a) bacteria and b) fungi under treatments: CK (no amendment), MF (compost plus NPK fertilizer), B (biochar), B1MF (biochar-based fertilizer at half of the biochar amount in B), BMF (biochar-based fertilizer at B) and B4MF (biochar-based fertilizer at double the amount of biochar in B).

(Fig. 2a, b). The total variance explained by the first two axes (PC1 and PC2) were 47.51% and 47.16% of bacterial and fungal communities under the six treatments sampled, respectively (Fig. 2). Based on the Bray Curtis distance algorithm, hierarchical clustering trees on the OTU level of all samples demonstrated that the bacterial and fungal community structures could be classified into three groups, namely, the no-biochar treated group (CK and MF), the low_carbon-biochar treated group (B and B1MF), and the high_carbon-biochar treated group (BMF and B4MF) (Fig. 3a, b). The bacterial and fungal PERMANOVA of the Bray Curtis analysis demonstrated a significant difference between treatments of soil bacterial and fungal samples ($P < 0.01$; Table S2), respectively, and revealed a significant difference between treated groups of soil bacterial and fungal samples, respectively ($P < 0.01$; Table S2).

3.4. Indicator microbes for each treated group

Indicator microbes are the specialized communities that represent microbial communities with statistically significant differences (Huhe et al., 2017). The LEfSe tool was employed to analyze the compositions of bacterial and fungal communities. The taxa for each treated group were displayed in the cladogram (Fig. 4a, b). The indicator bacteria of the no-biochar (CK_MF) group were of the orders *Blastocatellales* (belonging to phylum *Acidobacteria*) and *Solirubrobacterales* (belonging to phylum *Actinobacteria*) and the phylum *Firmicutes* (including class *Bacilli* and family *Bacillaceae*). Those of the low_carbon-biochar (B_B1MF) group were phyla *Actinobacteria* (including orders *Acidimicrobiales*, *Propionibacteriales*, and *Solirubrobacterales*) and *Proteobacteria* (including orders *Rhizobiales* and *Rhodospirillales*). Those of the high_carbon-biochar (BMF_B4MF) group were phyla *Actinobacteria* (including order *Gaiellales*), *Bacteroidetes* (including classes *Flavobacteriia* and *Sphingobacteriia*) and *Proteobacteria* (including classes *Alphaproteobacteria* and *BetaProteobacteria*) (Fig. 4a). The indicator fungi of the no-biochar group were the phylum *Ascomycota* (including classes *Dothideomycetes* and *Sordariomycetes*), family *Agaricaceae* (belonging to phylum *Basidiomycota*), and phylum *Mortierellomycota* (including class *Mortierellomycetes* and family *Mortierellaceae*). Those of the low_carbon-biochar group were phylum *Ascomycota* (including classes *Archaeorhizomycetes*, *Eurotiomycetes*, *Pezizomycetes*, and *Sordariomycetes*). Those of the high_carbon-biochar group were phylum *Ascomycota* (including classes *Eurotiomycetes* and *Sordariomycetes*) and class *Agaricomycetes* (belonging to phylum *Basidiomycota*) (Fig. 4b). The indicator microbes with linear discriminant analysis (LDA) threshold at 3.5 in bacterial and fungal communities associated with each group are presented in Fig. S2a and b, respectively.

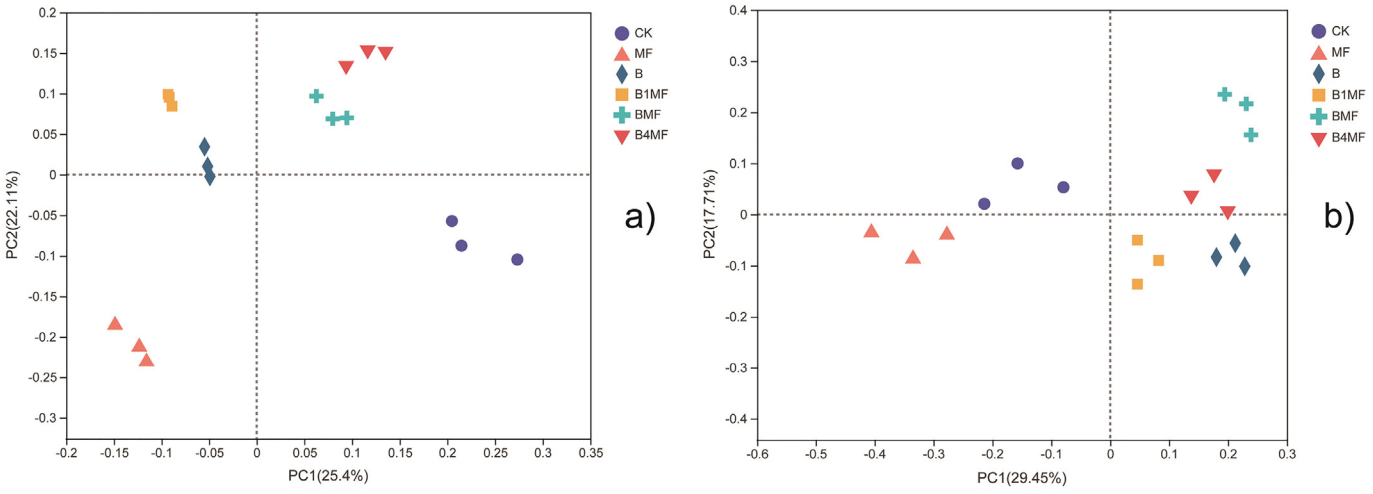

Fig. 2. The PCoA of a) bacterial community and b) fungal community. The PCoA plots were based on the spearman_approx distance at the OTU level (97% sequence similarity) of bacterial and fungal communities, respectively.

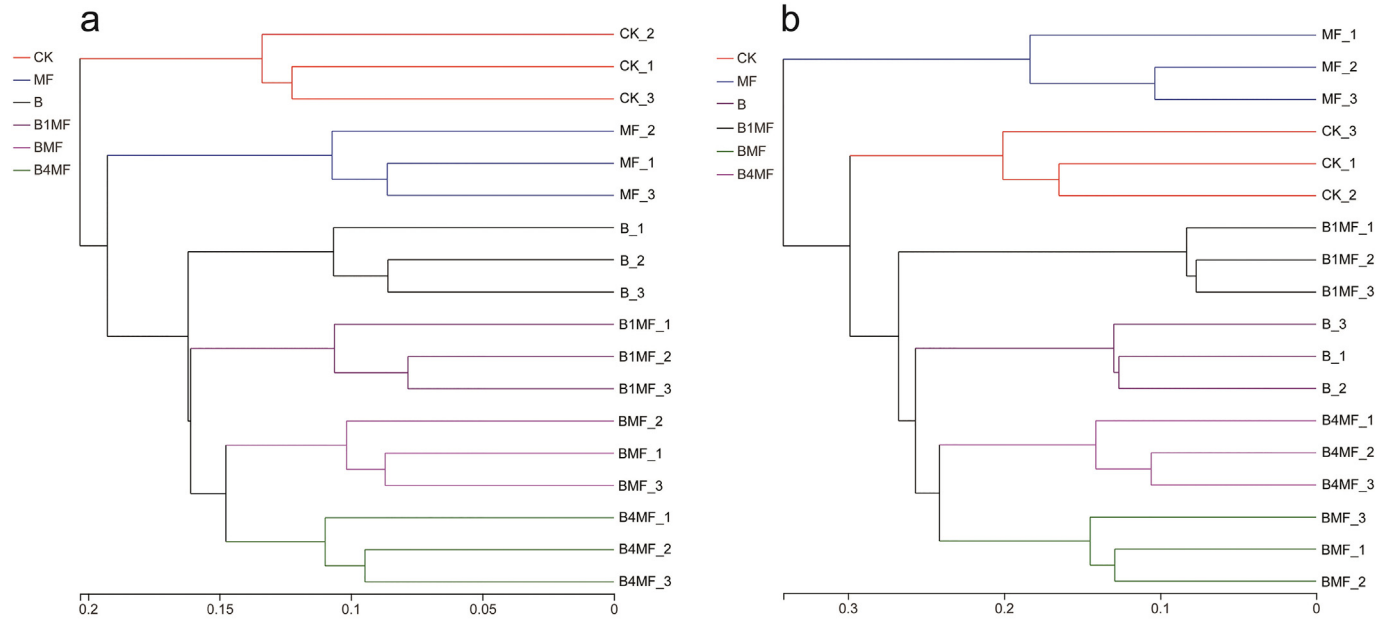

Fig. 3. Herarchical clustering trees of a) bacterial and b) fungal communities on OTU level (97% sequence similarity) under treatments of CK, MF, B, B1MF, BMF and B4MF.

3.5. Relationship between microbial community structure and soil properties

The RDA of the relationship between microbial communities at the phylum level and the soil physicochemical properties sufficiently explained the changes in soil bacterial and fungal community structures. The first two axes of the RDA model accounted for 57.04% and 74.71% of the total variance in the bacterial and fungal communities, respectively (Fig. 5a, b). According to the Mantel test (Table 3), SOC,

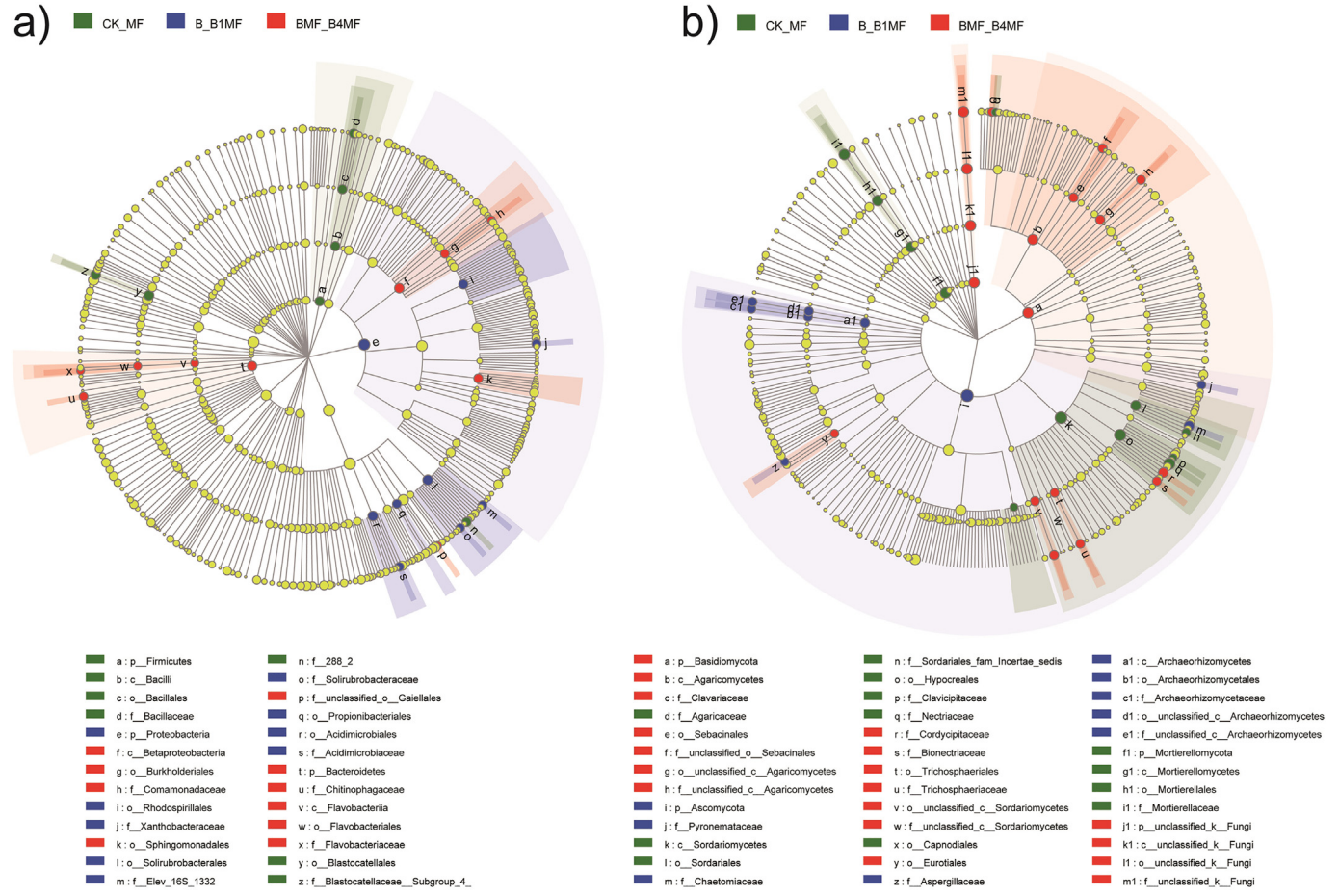

Fig. 4. LEfSe analysis of each treated group in a) bacterial community and b) fungal community. Cladograms showed the phylogenetic distribution of bacterial and fungal lineages associated with soils from the three treated groups.

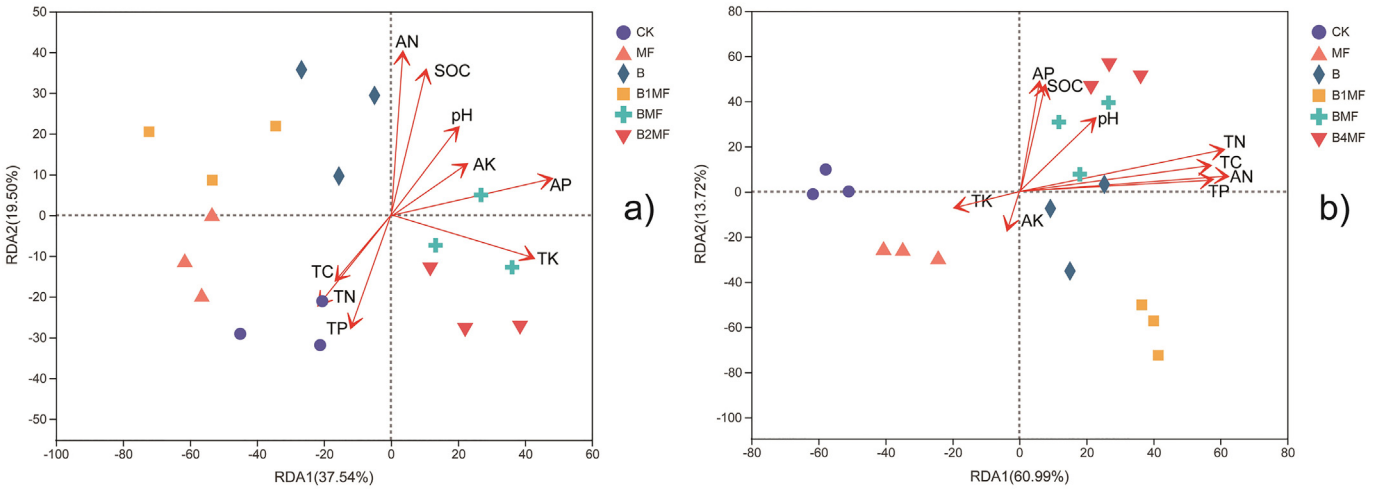

Fig. 5. RDA analysis of the relationship between microbial communities at the phylum level and the soil physicochemical properties. a) bacterial community, b) fungal community.

AN, and AP significantly influenced the bacterial community structure, while the TC, TN, TP, SOC, AN, and AP significantly influenced the fungal community structure. A Pearson's correlation analysis between the bacterial community and soil variables indicated that the relative abundance of phylum *Actinobacteria* was significantly positively correlated with the TP ($P < 0.01$), SOC ($P < 0.01$), AN ($P < 0.05$), and AP ($P < 0.01$), while the relative abundance of phylum *Proteobacteria* was significantly positively correlated with the SOC ($P < 0.05$), AN ($P < 0.05$), AP ($P < 0.01$), and AK ($P < 0.05$) (Fig. 6a). A Pearson's correlation analysis between the fungal community and soil variables displayed that the relative abundance of phylum *Ascomycota* was significantly positively correlated with the TC ($P < 0.01$), TN ($P < 0.01$), TP ($P < 0.001$), AN ($P < 0.001$), and AP ($P < 0.01$), while the relative abundance of phylum *Mortierellomycota* was significantly positively correlated with the pH ($P < 0.05$), TC ($P < 0.01$), TN ($P < 0.001$), TP ($P < 0.05$), SOC ($P < 0.05$), AN ($P < 0.05$), and AP ($P < 0.01$) (Fig. 6b).

3.6. Co-occurrence network structure of soil microbial communities

Based on dividing the treatments into three treated groups, three networks were constructed, namely, the no-biochar network, the low_carbon-biochar network, and the high_carbon-biochar network (Fig. 7). The quantities of total nodes and total links in the high_carbon-biochar network were higher than the two other networks, indicating that the high_carbon-biochar network was more complex than the two other networks (Fig. 7; Table 4). Additionally, the high_carbon-biochar network had a higher average degree and average clustering coefficient than the other two networks, suggesting that the high_carbon-biochar network was the most complex network among the three networks (Table 4). According to the number of links, average degree, and average clustering coefficient, the low_carbon-biochar network was more complex than the no-biochar network. The number of positive links in the no-biochar, low_carbon-biochar, and high_carbon-biochar networks were 219, 253 and 283, respectively, accounting for 62.9%, 69.3%, and 56.1% of the total number of corresponding links, suggesting that positive co-occurrence patterns predominated in the corresponding network (Fig. 7, Table 4). The number of negative links in the no-biochar, low_carbon-biochar, and high_carbon-biochar networks were 129, 112 and 221, respectively, accounting for 37.1%, 30.7%, and 43.8% of the total number of corresponding links, indicating a more competitive correlation among microbes in the high_carbon-biochar network (Fig. 7, Table 4). The no-biochar network had a lower average path distance and modularity than the other two networks, indicating that the no-biochar network was more susceptible to interference from the external environment than the other two networks, while the high_carbon-biochar network was more stable than the other two networks (Table 4). There were 21 bacterial and 5 fungal keystone species in the no-biochar network, namely, 11 bacterial keystone species from phylum *Actinobacteria*, 1 bacterial keystone species from phylum *Chloroflexi*, 1 bacterial keystone species from phylum *Firmicutes*, 1 bacterial keystone species from phylum *Nitrospirae*, 7 bacterial keystone species from phylum *Proteobacteria*, and 5 fungal keystone species from phylum *Ascomycota* (Table S3). The low_carbon-biochar network had a total of 23 bacterial and 6 fungal keystone species, namely, 3 bacterial keystone species from phylum *Acidobacteria*, 11 bacterial keystone species from phylum *Actinobacteria*, 1 bacterial keystone species from phylum *Chloroflexi*, 1 bacterial keystone species from phylum *Firmicutes*, 7 bacterial keystone species from phylum *Proteobacteria*, 5 fungal keystone species from phylum *Ascomycota*, and 1 fungal keystone species from phylum *Mortierellomycota* (Table S3). A total of 36 bacterial and 9 fungal keystone species were contained in the high_carbon-biochar network, namely, 6 bacterial keystone species from phylum *Acidobacteria*, 12 bacterial keystone species from phylum *Actinobacteria*, 1 bacterial keystone species from phylum *Bacteroidetes*, 1 bacterial keystone species from phylum *Nitrospirae*, 15 bacterial keystone species from phylum *Proteobacteria*, 1 bacterial keystone species from phylum *Verrucomicrobia*, 8 fungal keystone species from phylum *Ascomycota*, and 1 fungal keystone species from phylum *Mortierellomycota* (Table S3).

Table 3
Relationships between microbial community structure and environmental variables as revealed by Mantel.

Soil variables	Bacteria		Fungi	
	Mantel r statistic	*P*-value	Mantel r statistic	*P*-value
pH	0.068	0.093	0.291	0.065
TC	0.124	0.303	0.302*	0.014
TN	0.210	0.101	0.163**	0.009
TP	0.086	0.579	0.091*	0.036
TK	0.185	0.118	0.083	0.509
SOC	0.386*	0.025	0.297**	0.001
AN	0.115**	0.006	0.339**	0.004
AP	0.263*	0.017	0.128*	0.041
AK	0.072	0.926	0.046	0.686

The Mantel tests were conducted based on 9999 permutations between microbial community structure (Bray-Curtis distance) and soil variables (Euclidean distance). The symbols * and ** represent statistically significant differences at the 0.05 level and 0.01 level, respectively.

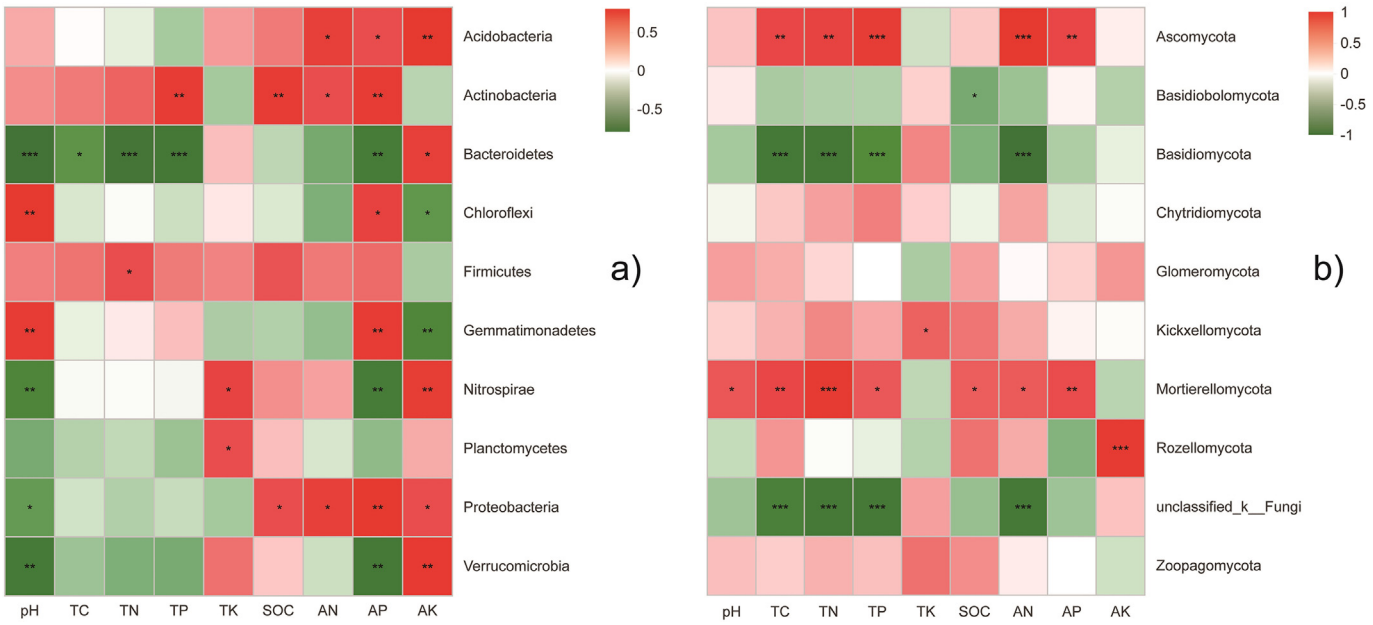

Fig. 6. Pearson's correlation analysis between the microbial community and soil variables. a) bacterial community, b) fungal community. *, $P < 0.05$; **, $P < 0.01$; ***, $P < 0.001$.

4. Discussion

4.1. Alterations in composition and structure of microbial community

The addition of biochar led to increased bacterial and fungal diversity, which indicated that the microbial community diversity increased. This change is mainly due to the high porosity of biochar, which provides habitats for microorganisms, protecting them from predators and increasing niches that support more microbial diversity (Lehmann et al., 2011). The micrographs of scanning electron microscopy revealed that bacteria and fungi could colonize the biochar pores (Lehmann et al., 2011). In the manufacturing process of biochar, the pyrolysis of biomass feedstock can convert several nutrients so that they can be used for microbial metabolism (Ameloot et al., 2013). Additionally, the biochar pore structure makes biochar have a larger specific surface area, allowing more chemical functional groups to adhere to the biochar, thus increasing its physical and chemical adsorption of soil nutrients, which in turn can be utilized by microorganisms (Hanzel et al., 2013). Furthermore, the addition of biochar can improve the soil environment, for example, by increasing soil nutrient content, cation exchange capacity, and water holding capacity, which can indirectly affect the diversity and structure of the soil microbial community (Yao et al., 2017). This was evidenced by the increase in soil nutrients following the addition of biochar to karst soil (Table 1). Generally, biochar contains many recalcitrant carbons that most microorganisms cannot utilize (Lehmann et al., 2011). With its higher content of microbial organic resources, compost can offer supplemental metabolic nutrients to soil microorganisms and support the modulation of soil microbial community structure (Bei et al., 2018). Biochar plus compost and fertilizer (BMF and B4MF) treated soils had significantly higher pH and nutrients than CK, MF and B treated soils ($P < 0.05$; Table 1). This indicates that the combination of these three components has the potential to improve soil properties.

The relative bacterial abundance of the phylum *Actinobacteria* was higher than the other phyla in each treatment (Fig. 1a). Furthermore, the relative abundances of the phylum *Actinobacteria* significantly increased in the BMF and B4MF compared to the other treatments ($P < 0.05$; Fig. S1a). Members of the phylum *Actinobacteria* are suitable for managing a large variety of carbon sources, and played an important role in the biogeochemical cycling of soil carbon, particularly in the presence of recalcitrant biochar (Lehmann et al., 2011). This may be why the indicator bacteria in the three treated groups (CK_MF, B_B1MF, and BMF_B4MF) all contained members of the phylum *Actinobacteria* (Fig. 4a). Moreover, this sufficiently explained why the soil organic carbon contents under BMF and B4MF treatments were significantly higher than other treatments (Table 1). The phylum *Proteobacteria* was also among the dominant bacterial species under each treatment (Fig. 1a). Additionally, it was the indicator bacteria of both the low_carbon-biochar group and high_carbon-biochar group (Fig. 4a). The members of *Proteobacteria* have been reported to play an important role in the circulation of soil nutrients in organic matter-rich environments (Ren et al., 2018). They could play a dominant role in organic phosphate solubilization and soil nitrogen fixation (Long et al., 2018), which could help solubilize the rich organic matter introduced by biochar and compost in the BMF and B4MF treatments. Thus, the contents of available nitrogen and available phosphorous in BMF- and B4MF-treated soils were significantly higher than those in other treated soils (Table 1).

The phylum *Ascomycota* was the most abundant fungal community in each treatment, and its members were the indicator fungi in each group (CK_MF, B_B1MF, and BMF_B4MF) (Figs. 1b; 4b). This result was consistent with Chen et al. (2017), who found that the fungal community was often predominated by *Ascomycota* under the environmental stress with drought and lack of nutrients or carbon. As we generally know, the environmental stress of the karst mountainous ecosystem in southwestern China is mainly due to the seasonal drought and barren karst soils (Liu et al., 2015a, 2015b; Gu et al., 2015). Meanwhile, *Ascomycota* played an important role in the degradation of compost (Yu et al., 2015; Duan et al., 2019). Compost application combined with biochar can change the relative abundance of *Ascomycota*, while raising the ratio of biochar in the mixture of compost and biochar can gradually increase the abundance of *Ascomycota* (Duan et al., 2019; Li et al., 2020a, 2020b). This finding sufficiently explained why the treatments in descending order of *Ascomycota* abundance were B4MF, BMF, B1MF, and MF (Figs. 1b; S1b). In contrast, the relative abundance of the phylum *Basidiomycota* gradually decreased in the order of no-biochar, low_carbon-biochar and high_carbon-biochar groups (Fig. 1b). This may be due to phyla *Basidiomycota* responding in contrasting ways to environmental stress (Sterkenburg et al., 2015; Tedersoo et al., 2016). As aerobic fungi, *Basidiomycota* can survive in anaerobic conditions (Li et al., 2020a, 2020b). Compost without biochar addition (CK_MF) formed many anaerobic pockets to proliferate a larger quantity of

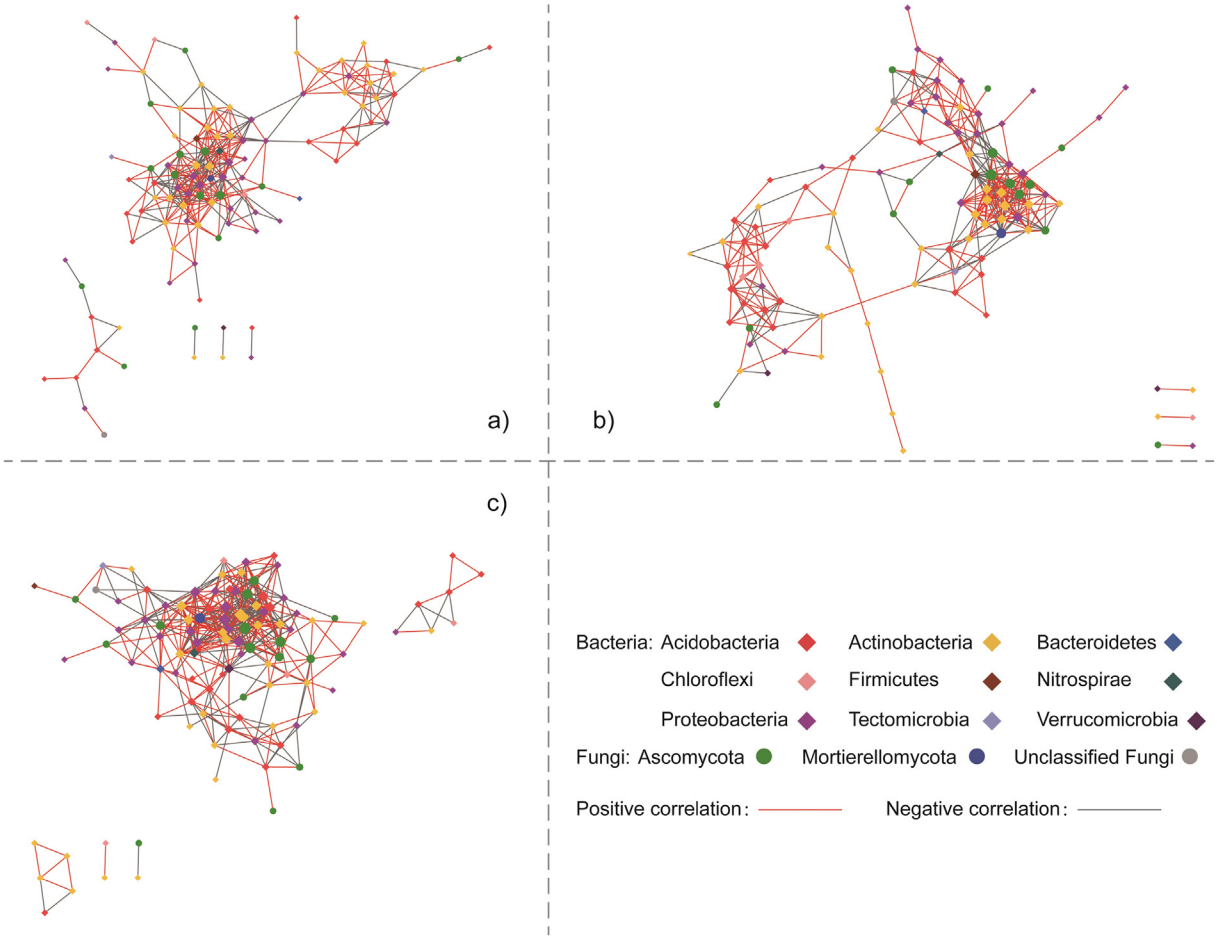

Fig. 7. Molecular ecological networks of bacterial and fungal communities within three treated groups. a) no-biochar network, b) low_carbon-biochar network and c) high_carbon-biochar network. Squares and circles are sized according to the connectivity degree of the nodes. Node colors represent the OTU taxa at the phylum level.

Basidiomycota (Li et al., 2020a, 2020b). This also resulted in *Basidiomycota* becoming an indicator fungus in the CK_MF group (Fig. 4b). Moreover, the BMF_B4MF group had *Basidiomycota* as an indicator fungus (Fig. 4b). It was reported that *Basidiomycota* could degrade organic pollutants (Weiland-Bräuer et al., 2017). The BMF_B4MF group contained the maximum number of organic pollutants (Sheng and Zhu, 2018), such as polycyclic aromatic hydrocarbons (PAHs), which were introduced by a larger quantity of biochar, resulting in *Basidiomycota* as an indicator fungus existing in this group. Additionally, the relative abundance of *Mortierellomycota* was increased by soil amendments (Fig. 1b). With the addition of soil amendments, the soil became rich in nutrients, providing suitable habitat for *Mortierellomycota* (Zhao et al., 2016; Cong et al., 2020). Morever, as saprophytic fungi, members of the phylum *Mortierellomycota* could benefit from the compost addition. This was confirmed by Cong et al. (2020). Furthermore, these findings sufficiently explained why the phylum *Mortierellomycota* was the indicator fungus of the CK_MF group. Additionally, the B_B1MF and BMF_B4MF groups did not contain the indicator *Mortierellomycota* (Fig. 4b). This may be due to the addition of biochar, which introduced several toxic compounds such as PAHs that inhibited the activity of *Mortierellomycota* (Qian and Chen, 2014; Sheng and Zhu, 2018).

Table 4
Main properties of the co-occurrence network along with treatments of the no-biochar group (CK and MF), low_carbon-biochar group (B and B1MF) and high_carbon-biochar group (BMF and B4MF).

Network indexes	No-biochar	Low_carbon-biochar	High_carbon-biochar
Total nodes	104	104	106
Total links	348	365	504
Positive links	219	253	283
Negative links	129	112	221
Average degree	6.69*	7.14*	9.51*
Average clustering coefficient	0.42*	0.475*	0.529*
Average path distance	2.96*	3.81*	4.60*
Modularity	0.404*	0.506*	0.548*

The symbol * represents a statistically significant difference (0.05 level) between the three networks.

4.2. Correlations between microbial community structure and soil properties

The RDA results revealed that soil properties contributed more than 50% of the alterations in the composition of the microbial community (Fig. 5), suggesting that these soil environmental factors played a dominant role in constructing the structure of the microbial community. This result was confirmed by numerous studies (Zhang et al., 2016; Guo et al., 2019). According to Pearson's correlation analysis, several soil variables such as soil organic carbon and available nutrients demonstrated significant positive correlations with the predominant microbial communities (including *Actinobacteria*, *Proteobacteria*, *Ascomycota*, and *Mortierellomycota*) (Fig. 6). It was reported that these dominant microbial communities were responsible for soil carbon and nutrient cycling (Read and Perez-Moreno, 2003; Li et al., 2019a, 2019b; Li et al., 2020a, 2020b).

Phyla *Actinobacteria* and *Proteobacteria* were significantly and positively correlated with SOC, AN, and AP (Fig. 6a). *Actinobacteria* and *Proteobacteria* were reported to be involved in soil organic matter decomposition, N-cycling, and P-cycling (Ibrahim et al., 2020; Xue et al.,

2020). Additionally, phyla *Ascomycota* and *Mortierellomycota*, as saprophytic fungi, played dominant roles in the decomposition of soil organic matter (Li et al., 2019a, 2019b; Guo et al., 2019; Cong et al., 2020). Meanwhile, *Ascomycota* and *Mortierellomycota* had strong relationships with soil C, N and P fractions (Fig. 6b), which indicated that they played important roles in soil C-, N- and P-cycling. Furthermore, large quantities of organic matter and nutrients were introduced into the soil via soil amendments. Therefore, the soil nutrient status was improved by the biochar and compost addition (Table 1). Our study elucidated that the dominant microbial communities were positively correlated with several soil nutrients (AN and AP) and were sensitive to soil C fractions (TC or SOC) (Figs. 5; 6). Therefore, under the combined application of biochar plus organic manure and chemical fertilizer, the dominant bacteria and fungi thrived and played important roles in improving karst soils. However, to further determine the direct effects of soil environmental variables on microbial communities, a trait-based approach should be considered for future research (Rath et al., 2019; Wei et al., 2020). For example, the distributions of soil physicochemical traits within the microbial communities can be quantified through dose-response relationships between the soil variables and microbial growth.

4.3. Shifts of structure in co-occurrence network

In natural habitats, species cannot survive on their own; they form complex network systems through interactions between species (Liu et al., 2015a, 2015b). The concept of ecological networks was developed and widely used in studies of the food web, pollination network, and protein metabolism network (Krause et al., 2003; Guimera and Amaral, 2005; Olesen et al., 2008). In recent years, researchers have discovered that the secretion of metabolites by microorganisms can promote or inhibit the growth of other microorganisms (Marx, 2009), and this interaction between microorganisms is also consistent with the ecological network model (Peura et al., 2015).

Biochar-based fertilizer addition increased the complexity of microbial co-occurrence networks (Fig. 7; Table 4). This was reflected in the increased numbers of nodes, links, average degree and average clustering coefficient due to the addition of biochar-based fertilizer (Banerjee et al., 2019). Additionally, modularity was crucial for microbial community stability and resilience because it represented the microbial interactions, such as resource partitioning, habitat heterogeneity, phylogenetic correlations, or niche overlap (Olesen et al., 2007). Therefore, with the addition of biochar-based fertilizer, the increase of modularity implied higher microbial diversity (Yu et al., 2018). This was consistent with our results (Table 2). The increase of negative links indicated that the competition between microorganisms was more intense (Shi et al., 2016). This may be due to the higher quantity of organic matter that was introduced by more biochar, which promoted microorganisms to be more active, and produce more metabolites that inhibited the activity of other microorganisms, resulting in more competition between microorganisms (Hu et al., 2017).

The keystone taxa from modules within the soil microbial network usually represented the functional microbial communities responsible for nutrient cycling (Zhou et al., 2010). Because keystone taxa played specific roles in the circulation of different substances in the soil, the addition of biochar could lead to greater network complexity by providing more complex organic matters to soil microorganisms. (Yu et al., 2018) have found that the microbial community complexity increased after applying biochar to crop soils. High mean degree nodes, network hubs, connectors, and module hubs were the critical factors in microbial community function and network stability (Deng et al., 2012; Berry and Widder, 2014), and they were identified as the keystone taxa in a network (Shi et al., 2016). Once keystone taxa disappear, the original network topology structure would be decomposed (Faust and Raes, 2012). Meanwhile, based on the free scale property of the soil microbial network, this structure would be easily damaged due to soil environmental shifts (Steele et al., 2011). We speculate that the number of keystone taxa was positively correlated with the stability of the network structure. Due to the incremental numbers of keystone taxa, the network stability gradually increased in the order of low_carbon-biochar and high_carbon-biochar networks compared to the no-biochar network (Fig. 7, Table S3). To summarize, the higher microbial community diversity and more developed microbial co-occurrence network implied the increased soil ecosystem functions related to C- and nutrient-cycling. This has also been suggested by Wagg et al. (2019).

5. Conclusions

Soil amendments significantly changed the composition and structure of the soil microbial community in the karst mountainous area. The addition of biochar and biochar-based fertilizer to karst soil expanded the scale and complexity of the soil microbial network. Furthermore, biochar-based fertilizer addition enabled keystone taxa in the network topology structure to actively participate in soil carbon resource management and soil nutrient cycling. The contents of organic carbon and available nutrients were the highest in BMF- and B4MF-treated soils, indicating that the combined application of biochar plus organic manure and chemical fertilizer could perform better in the karst mountainous area.

CRediT authorship contribution statement

Taotao Yan: Data curation, Software, Writing – original draft. **Jianhui Xue:** Methodology, Conceptualization. **Zhidong Zhou:** Writing – review & editing. **Yongbo Wu:** Supervision.

Declaration of competing interest

The authors declare that they have no known competing financial interests or personal relationships that could have appeared to influence the work reported in this paper.

Acknowledgements

This work received funding from two organizations: a) Major State Basic Research Development Program of China under grant no. 2016YFC0502605 and b) Priority Academic Program Development of Jiangsu Higher Education Institutions under grant no. PAPD.

Appendix A. Supplementary data

Supplementary data to this article can be found online at https://doi.org/10.1016/j.scitotenv.2021.148757.

References

Alburquerque, J.A., Calero, J.M., Barrón, V., Torrent, J., Del Campillo, M.C., Gallardo, A., Villar, R., 2014. Effects of biochars produced from different feedstocks on soil properties and sunflower growth. J. Plant Nutr. Soil Sci. 177, 16–25.

Ameloot, N., Graber, E.R., Verheijen, F.G.A., De Neve, S., 2013. Interactions between biochar stability and soil organisms: review and research needs. Eur. J. Soil Sci. 64, 379–390.

Ao, T., Ran, Y., Chen, Y., Li, R., Luo, Y., Liu, X., Li, D., 2020. Effect of viscosity on process stability and microbial community composition during anaerobic mesophilic digestion of Maotai-flavored distiller's grains. Bioresour. Technol. 297.

Atkinson, C.J., Fitzgerald, J.D., Hipps, N.A., 2010. Potential mechanisms for achieving agricultural benefits from biochar application to temperate soils: a review. Plant Soil 337, 1–18.

Bai, S.H., Reverchon, F., Xu, C., Xu, Z., Blumfield, T.J., Zhao, H., Van Zwieten, L., Wallace, H.M., 2015. Wood biochar increases nitrogen retention in field settings mainly through abiotic processes. Soil Biol. Biochem. 90, 232–240.

Banerjee, S., Walder, F., Buechi, L., Meyer, M., Held, A.Y., Gattinger, A., Keller, T., Charles, R., van der Heijden, M.G.A., Agricultural intensification reduces microbial network complexity and the abundance of keystone taxa in roots, ISME J., 13 (2019), pp. 1722–1736.

Bei, S., Zhang, Y., Li, T., Christie, P., Li, X., Zhang, J., 2018. Response of the soil microbial community to different fertilizer inputs in a wheat-maize rotation on a calcareous soil. Agric. Ecosyst. Environ. 260, 58–69.

Berry, D., Widder, S., 2014. Deciphering microbial interactions and detecting keystone species with co-occurrence networks. Front. Microbiol. 5.
Chan, K., Xu, Z., 2009. Biochar: Nutrient properties and their enhancement. Biochar for Environmental Management: Science, Technology and Implementation, pp. 67–84.
Chen, H., Liu, J., Wang, K., Zhang, W., 2011. Spatial distribution of rock fragments on steep hillslopes in karst region of northwest Guangxi, China. Catena 84, 21–28.
Chen, Y., Xu, T., Veresoglou, S.D., Hu, H., Hao, Z., Hu, Y., Liu, L., Deng, Y., Rillig, M.C., Chen, B., 2017. Plant diversity represents the prevalent determinant of soil fungal community structure across temperate grasslands in northern China. Soil Biol. Biochem. 110, 12–21.
Chintala, R., Schumacher, T.E., McDonald, L.M., Clay, D.E., Malo, D.D., Papiernik, S.K., Clay, S.A., Julson, J.L., 2014. Phosphorus sorption and availability from biochars and soil/biochar mixtures. CLEAN - Soil Air Water 42, 626–634.
Chun, Y., Sheng, G., Chiou, C.T., Xing, B., 2004. Compositions and sorptive properties of crop residue-derived chars. Environ. Sci. Technol. 38, 4649–4655.
Cong, P., Wang, J., Li, Y., Liu, N., Dong, J., Pang, H., Zhang, L., Gao, Z., 2020. Changes in soil organic carbon and microbial community under varying straw incorporation strategies. Soil Tillage Res. 204, 104735.
Deluca, T., Mackenzie, M.D., Gundale, M.J., Biochar Effects on Soil Nutrient Transformations, Earthscan Publications Ltd., London, UK, 2009.
Deng, Y., Jiang, Y., Yang, Y., He, Z., Luo, F., Zhou, J., 2012. Molecular ecological network analyses. BMC Bioinformatics 13, 113.
Ding, Y., Liu, Y., Wu, W., Shi, D., Yang, M., Zhong, Z., 2010. Evaluation of biochar effects on nitrogen retention and leaching in multi-layered soil columns. Water Air Soil Pollut. 213, 47–55.
Duan, Y., Awasthi, S.K., Liu, T., Chen, H., Zhang, Z., Wang, Q., Ren, X., Tu, Z., Awasthi, M.K., Taherzadeh, M.J., 2019. Dynamics of fungal diversity and interactions with environmental elements in response to wheat straw biochar amended poultry manure composting. Bioresour. Technol. 274, 410–417.
Dumroese, R.K., Heiskanen, J., Englund, K., Tervahauta, A., 2011. Pelleted biochar: chemical and physical properties show potential use as a substrate in container nurseries. Biomass Bioenergy 35, 2018–2027.
Fan, D., Zhang, Y., Qin, S., Wu, B., 2017. Relationships between Artemisia ordosica communities and environmental factors following sand-dune stabilization in the Mu Us desert, northwest China. J. For. Res. 28, 115–124.
Faust, K., Raes, J., 2012. Microbial interactions: from networks to models. Nat. Rev. Microbiol. 10, 538–550.
Fierer, N., 2017. Embracing the unknown: disentangling the complexities of the soil microbiome. Nat. Rev. Microbiol. 15, 579–590.
Ford, D.C., Williams, P.W., 2007. Karst Hydrogeology and Geomorphology. 2nded. Wiley, London.
Fungo, B., Lehmann, J., Kalbitz, K., Thionġo, M., Okeyo, I., Tenywa, M., Neufeldt, H., 2017. Aggregate size distribution in a biochar-amended tropical Ultisol under conventional hand-hoe tillage. Soil Tillage Res. 165, 190–197.
Gaunt, J.L., Lehmann, J., 2008. Energy balance and emissions associated with biochar sequestration and pyrolysis bioenergy production. Environ. Sci. Technol. 42, 4152–4158.
Gu, D., Zhang, Z., Mallik, A., Zhou, A., Mo, L., He, C., Huang, Y., 2015. Seasonal water use strategy of Cyclobalanopsis glauca in a karst area of southern China. Environ. Earth Sci. 74, 1007–1014.
Guimera, R., Amaral, L., 2005. Functional cartography of complex metabolic networks. Nature 433, 895–900.
Guo, J., Wang, G., Wu, Y., Shi, Y., Feng, Y., Cao, F., Ginkgo agroforestry practices alter the fungal community structures at different soil depths in eastern China, Environ. Sci. Pollut. Res., 26 (2019), pp. 21253–21263.
Hammer, E.C., Balogh-Brunstad, Z., Jakobsen, I., Olsson, P.A., Stipp, S.L.S., Rillig, M.C., 2014. A mycorrhizal fungus grows on biochar and captures phosphorus from its surfaces. Soil Biol. Biochem. 77, 252–260.
Hanzel, J., Myrold, D., Sessitsch, A., Smalla, K., Tebbe, C.C., Totsche, K.U., Microbial ecology of biogeochemical interfaces - diversity, structure, and function of microhabitats in soil, FEMS Microbiol. Ecol., 86 (2013), pp. 1–2.
Horvath, S., Dong, J., 2008. Geometric interpretation of gene coexpression network analysis. PLoS Comput. Biol. 4, e1000117.
Hu, X., Liu, J., Wei, D., Zhu, P., Cui, X., Zhou, B., Chen, X., Jin, J., Liu, X., Wang, G., 2017. Effects of over 30-year of different fertilization regimes on fungal community compositions in the black soils of northeast China. Agric. Ecosyst. Environ. 248, 113–122.
Huhe Chen, X., Hou, F., Wu, Y., Cheng, Y., 2017. Bacterial and fungal community structures in loess plateau grasslands with different grazing intensities. Front. Microbiol. 8.
Ibrahim, M.M., Tong, C., Hu, K., Zhou, B., Xing, S., Mao, Y., 2020. Biochar-fertilizer interaction modifies N-sorption, enzyme activities and microbial functional abundance regulating nitrogen retention in rhizosphere soil. Sci. Total Environ. 739.
Jeffries, P., Gianinazzi, S., Perotto, S., Turnau, K., Barea, J., The contribution of arbuscular mycorrhizal fungi in sustainable maintenance of plant health and soil fertility, Biol. Fertil. Soils, 37 (2003), pp. 1–16.
Jiang, Z., Lian, Y., Qin, X., 2014. Rocky desertification in Southwest China: impacts, causes, and restoration. Earth-Sci. Rev. 132, 1–12.
Kõljalg, U., Larsson, K., Abarenkov, K., Nilsson, R.H., Alexander, I.J., Eberhardt, U., Erland, S., Høiland, K., Kjøller, R., Larsson, E., Pennanen, T., Sen, R., Taylor, A.F.S., Tedersoo, L., Vrålstad, T., UNITE: a database providing web-based methods for the molecular identification of ectomycorrhizal fungi, New Phytol., 166 (2005), pp. 1063–1068.
Krause, A.E., Frank, K.A., Mason, D.M., Ulanowicz, R.E., Taylor, W.W., 2003. Compartments revealed in food-web structure. Nature 426, 282–285.
Kuzyakov, Y., Subbotina, I., Chen, H., Bogomolova, I., Xu, X., 2009. Black carbon decomposition and incorporation into soil microbial biomass estimated by 14C labeling. Soil Biol. Biochem. 41, 210–219.
Lehmann, J., Rillig, M.C., Thies, J., Masiello, C.A., Hockaday, W.C., Crowley, D., 2011. Biochar effects on soil biota – a review. Soil Biol. Biochem. 43, 1812–1836.
Li, Y., Li, Y., Chang, S.X., Yang, Y., Fu, S., Jiang, P., Luo, Y., Yang, M., Chen, Z., Hu, S., Zhao, M., Liang, X., Xu, Q., Zhou, G., Zhou, J., 2018. Biochar reduces soil heterotrophic respiration in a subtropical plantation through increasing soil organic carbon recalcitrancy and decreasing carbon degrading microbial activity. Soil Biol. Biochem. 122, 173–185.
Li, Y., Fang, F., Wei, J., Wu, X., Cui, R., Li, G., Zheng, F., Tan, D., 2019a. Humic acid fertilizer improved soil properties and soil microbial diversity of continuous cropping peanut: a three-year experiment. Sci. Rep.-UK 9.
Li, X., Shi, X., Lu, M., Zhao, Y., Li, X., Peng, H., Guo, R., 2019b. Succession of the bacterial community and functional characteristics during continuous thermophilic composting of dairy manure amended with recycled ceramsite. Bioresour. Technol. 294.
Li, J., Bao, H., Xing, W., Yang, J., Liu, R., Wang, X., Lv, L., Tong, X., Wu, F., 2020a. Succession of fungal dynamics and their influence on physicochemical parameters during pig manure composting employing with pine leaf biochar. Bioresour. Technol. 297, 122377.
Li, R., Li, Q., Zhang, J., Liu, Z., Pan, L., Huang, K., Zhang, L., 2020b. Effects of organic mulch on soil moistureand nutrients in karst area of Southwest China. Pol. J. Environ. Stud. 29, 4161–4174.
Liang, B., Lehmann, J., Solomon, D., Sohi, S., Thies, J.E., Skjemstad, J.O., Luizão, F.J., Engelhard, M.H., Neves, E.G., Wirick, S., 2008. Stability of biomass-derived black carbon in soils. Geochim. Cosmochim. Acta 72, 6069–6078.
Liang, Y., He, X., Chen, C., Feng, S., Liu, L., Chen, X., Zhao, Z., Su, Y., 2015. Influence of plant communities and soil properties during natural vegetation restoration on arbuscular mycorrhizal fungal communities in a karst region. Ecol. Eng. 82, 57–65.
Liu, J., Schulz, H., Brandl, S., Miehtke, H., Huwe, B., Glaser, B., 2012. Short-term effect of biochar and compost on soil fertility and water status of a Dystric Cambisol in NE Germany under field conditions. J. Plant Nutr. Soil Sci. 175, 698–707.
Liu, B., Chen, C., Lian, Y., Chen, J., Chen, X., 2015a. Long-term change of wet and dry climatic conditions in the southwest karst area of China. Glob. Planet. Chang. 127, 1–11.
Liu, J., Sui, Y., Yu, Z., Shi, Y., Chu, H., Jin, J., Liu, X., Wang, G., 2015b. Soil carbon content drives the biogeographical distribution of fungal communities in the black soil zone of northeast China. Soil Biol. Biochem. 83, 29–39.
Liu, C., Liu, Y., Guo, K., Wang, S., Liu, H., Zhao, H., Qiao, X., Hou, D., Li, S., 2016. Aboveground carbon stock, allocation and sequestration potential during vegetation recovery in the karst region of southwestern China: a case study at a watershed scale. Agric. Ecosyst. Environ. 235, 91–100.
Liu, Y., Zhu, J., Gao, W., Guo, Z., Xue, C., Pang, J., Shu, L., Effects of biochar amendment on bacterial and fungal communities in the reclaimed soil from a mining subsidence area, Environ. Sci. Pollut. Res. 26 (2019), pp. 34368–34376.
Long, X., Yao, H., Huang, Y., Wei, W., Zhu, Y., 2018. Phosphate levels influence the utilisation of rice rhizodeposition carbon and the phosphate-solubilising microbial community in a paddy soil. Soil Biol. Biochem. 118, 103–114.
Lu, R.K., 1999. Soil and Agro-Chemical Analytical Methods. China Agriculture Science and Technology Press, Beijing.
Luo, F., Yang, Y., Zhong, J., Gao, H., Khan, L., Thompson, D.K., Zhou, J., 2007. Constructing gene co-expression networks and predicting functions of unknown genes by random matrix theory. BMC Bioinformatics 8, 299.
Luo, X., Fu, X., Yang, Y., Cai, P., Peng, S., Chen, W., Huang, Q., Microbial communities play important roles in modulating paddy soil fertility, Sci. Rep.-UK, 6 (2016).
Macdonald, L.M., Farrell, M., Zwieten, L.V., Krull, E.S., 2014. Plant growth responses to biochar addition: an Australian soils perspective. Biol. Fertil. Soils 50, 1035–1045.
Manirakiza, E., Ziadi, N., St. Luce, M., Hamel, C., Antoun, H., Karam, A., Nitrogen mineralization and microbial biomass carbon and nitrogen in response to co-application of biochar and paper mill biosolids, Appl. Soil Ecol., 142 (2019), pp. 90–98.
Marris, E., 2006. Black is the new green. Nature 442, 624–626.
Marx, C.J., 2009. Getting in touch with your friends. Science 324, 1150–1151.
Newman, M.E.J., 2006. Modularity and community structure in networks. Proc. Natl. Acad. Sci. 103, 8577–8582.
Olesen, J.M., Bascompte, J., Dupont, Y.L., Jordano, P., 2007. The modularity of pollination networks. Proc. Natl. Acad. Sci. 104, 19891–19896.
Olesen, J.M., Bascompte, J., Elberling, H., Jordano, P., 2008. Temporal dynamics in a pollination network. Ecology 89, 1573–1582.
Olsen, S.R., 1954. Estimation of available phosphorus in soils by extraction with sodium bicarbonate., US Department of Agriculture. Circ 939.
Peura, S., Bertilsson, S., Jones, R.I., Eiler, A., 2015. Resistant microbial cooccurrence patterns inferred by network topology. Appl. Environ. Microbiol. 81, 2090–2097.
Pituello, C., Dal Ferro, N., Francioso, O., Simonetti, G., Berti, A., Piccoli, I., Pisi, A., Morari, F., 2018. Effects of biochar on the dynamics of aggregate stability in clay and sandy loam soils. Eur. J. Soil Sci. 69, 827–842.
Qian, L., Chen, B., 2014. Interactions of aluminum with biochars and oxidized biochars: implications for the biochar aging process. J. Agric. Food Chem. 62, 373–380.
Quast, C., Pruesse, E., Yilmaz, P., Gerken, J., Schweer, T., Yarza, P., Peplies, J., Gloeckner, F.O., The SILVA ribosomal RNA gene database project: improved data processing and web-based tools, Nucleic Acids Res., 41 (2013), pp. D590-D596.
Rath, K.M., Fierer, N., Murphy, D.V., Rousk, J., 2019. Linking bacterial community composition to soil salinity along environmental gradients. ISME J. 13, 836–846.
Read, D.J., Perez-Moreno, J., 2003. Mycorrhizas and nutrient cycling in ecosystems - a journey towards relevance? New Phytol. 157, 475–492.
Ren, C., Wang, T., Xu, Y., Deng, J., Zhao, F., Yang, G., Han, X., Feng, Y., Ren, G., Differential soil microbial community responses to the linkage of soil organic carbon fractions with respiration across land-use changes, Forest Ecol. Manag., 409 (2018), pp. 170–178.
Rex, D., Schimmelpfennig, S., Jansen-Willems, A., Moser, G., Kammann, C., Müller, C., 2015. Microbial community shifts 2.6 years after top dressing of Miscanthus biochar, hydrochar and feedstock on a temperate grassland site. Plant Soil 397, 261–271.

Roberts, K.G., Gloy, B.A., Joseph, S., Scott, N.R., Lehmann, J., 2010. Life cycle assessment of biochar systems: estimating the energetic, economic, and climate change potential. Environ. Sci. Technol. 44, 827–833.
Sauro, U., 1993. Human impact on the karst of the venetian fore-Alps, Italy. Environ. Geol. 21, 115–121.
Shade, A., Handelsman, J., 2012. Beyond the Venn diagram: the hunt for a core microbiome. Environ. Microbiol. 14, 4–12.
Shannon, P., Markiel, A., Ozier, O., Baliga, N.S., Wang, J.T., Ramage, D., Amin, N., Schwikowski, B., Ideker, T., Cytoscape: a software environment for integrated models of biomolecular interaction networks, Genome Res., 13 (2003), pp. 2498–2504.
Sheng, Y., Zhu, L., 2018. Biochar alters microbial community and carbon sequestration potential across different soil pH. Sci. Total Environ. 622-623, 1391–1399.
Shi, S., Nuccio, E.E., Shi, Z.J., He, Z., Zhou, J., Firestone, M.K., 2016. The interconnected rhizosphere: high network complexity dominates rhizosphere assemblages. Ecol. Lett. 19, 926–936.
Soil Survey Staff, 2014. Keys to Soil Taxonomy. USDA-Natural Resources Conservation Service, Washington, DC.
Steele, J.A., Countway, P.D., Xia, L., Vigil, P.D., Beman, J.M., Kim, D.Y., Chow, C.T., Sachdeva, R., Jones, A.C., Schwalbach, M.S., Rose, J.M., Hewson, I., Patel, A., Sun, F., Caron, D.A., Fuhrman, J.A., 2011. Marine bacterial, archaeal and protistan association networks reveal ecological linkages. ISME J. 5, 1414–1425.
Steiner, C., de Arruda, M.R., Teixeira, W.G., Zech, W., 2007. Soil respiration curves as soil fertility indicators in perennial central Amazonian plantations treated with charcoal, and mineral or organic fertilisers. Trop. Sci. 47, 218–230.
Sterkenburg, E., Bahr, A., Brandström Durling, M., Clemmensen, K.E., Lindahl, B.D., 2015. Changes in fungal communities along a boreal forest soil fertility gradient. New Phytol. 207, 1145–1158.
Tedersoo, L., Bahram, M., Cajthaml, T., Põlme, S., Hiiesalu, I., Anslan, S., Harend, H., Buegger, F., Pritsch, K., Koricheva, J., Abarenkov, K., 2016. Tree diversity and species identity effects on soil fungi, protists and animals are context dependent. ISME J. 10, 346–362.
Thies, J., Rillig, M., 2009. Characteristics of biochar: biological properties. Biochar for Environmental Management: Science and Technology, pp. 85–105.
Tian, J., Wang, J., Dippold, M., Gao, Y., Blagodatskaya, E., Kuzyakov, Y., 2016. Biochar affects soil organic matter cycling and microbial functions but does not alter microbial community structure in a paddy soil. Sci. Total Environ. 556, 89–97.
Tian, J., He, N., Kong, W., Deng, Y., Feng, K., Green, S.M., Wang, X., Zhou, J., Kuzyakov, Y., Yu, G., 2018. Deforestation decreases spatial turnover and alters the network interactions in soil bacterial communities. Soil Biol. Biochem. 123, 80–86.
Van Zwieten, L., Kimber, S., Morris, S., Chan, K.Y., Downie, A., Rust, J., Joseph, S., Cowie, A., 2010. Effects of biochar from slow pyrolysis of papermill waste on agronomic performance and soil fertility. Plant Soil 327, 235–246.
Wagg, C., Schlaeppi, K., Banerjee, S., Kuramae, E.E., van der Heijden, M.G.A., 2019. Fungal-bacterial diversity and microbiome complexity predict ecosystem functioning. Nat. Commun. 10.
Wang, J., Zou, B., Liu, Y., Tang, Y., Zhang, X., Yang, P., 2014. Erosion-creep-collapse mechanism of underground soil loss for the karst rocky desertification in Chenqi village, Puding county, Guizhou, China. Environ. Earth Sci. 72, 2751–2764.
Warnock, D.D., Lehmann, J., Kuyper, T.W., Rillig, M.C., 2007. Mycorrhizal responses to biochar in soil – concepts and mechanisms. Plant Soil 300, 9–20.
Warnock, D.D., Mummey, D.L., McBride, B., Major, J., Lehmann, J., Rillig, M.C., 2010. Influences of non-herbaceous biochar on arbuscular mycorrhizal fungal abundances in roots and soils: results from growth-chamber and field experiments. Appl. Soil Ecol. 46, 450–456.
Webster, R., 2008. Soil sampling and methods of analysis - edited by M.R. Carter & E.G. Gregorich. Eur. J. Soil Sci. 59, 1010–1011.
Wei, G., Li, M., Shi, W., Tian, R., Chang, C., Wang, Z., Wang, N., Zhao, G., Gao, Z., 2020. Similar drivers but different effects lead to distinct ecological patterns of soil bacterial and archaeal communities. Soil Biol. Biochem. 144.
Weiland-Bräuer, N., Fischer, M.A., Schramm, K., Schmitz, R.A., 2017. Polychlorinated biphenyl (PCB)-degrading potential of microbes present in a cryoconite of Jamtalferner glacier. Front. Microbiol. 8.
Williams, P., 1993. Environmental change and human impact on karst terrains. Catena (Suppl.25), 1–19.
Wu, H., Zeng, G., Liang, J., Chen, J., Xu, J., Dai, J., Li, X., Chen, M., Xu, P., Zhou, Y., Li, F., Hu, L., Wan, J., 2016. Responses of bacterial community and functional marker genes of nitrogen cycling to biochar, compost and combined amendments in soil. Appl. Microbiol. Biotechnol. 100, 8583–8591.
Xia, W., Jia, Z., 2014. Comparative analysis of soil microbial communities by pyrosequencing and DGGE. Acta Microbiol Sin. 54, 1489–1499.
Xu, G., Sun, J., Shao, H., Chang, S.X., Biochar had effects on phosphorus sorption and desorption in three soils with differing acidity, Ecol. Eng., 62 (2014), pp. 54–60.
Xu, N., Tan, G., Wang, H., Gai, X., 2016. Effect of biochar additions to soil on nitrogen leaching, microbial biomass and bacterial community structure. Eur. J. Soil Biol. 74, 1–8.
Xue, Y., Tian, J., Quine, T.A., Powlson, D., Xing, K., Yang, L., Kuzyakov, Y., Dungait, J.A.J., 2020. The persistence of bacterial diversity and ecosystem multifunctionality along a disturbance intensity gradient in karst soil. Sci. Total Environ. 748.
Yao, Q., Liu, J., Yu, Z., Li, Y., Jin, J., Liu, X., Wang, G., 2017. Three years of biochar amendment alters soil physiochemical properties and fungal community composition in a black soil of northeast China. Soil Biol. Biochem. 110, 56–67.
Yin, N., Zhang, Z., Wang, L., Qian, K., Variations in organic carbon, aggregation, and enzyme activities of gangue-fly ash-reconstructed soils with sludge and arbuscular mycorrhizal fungi during 6-year reclamation, Environ. Sci. Pollut. Res., 23 (2016), pp. 17840–17849.
Yu, M., Zhang, J., Xu, Y., Xiao, H., An, W., Xi, H., Xue, Z., Huang, H., Chen, X., Shen, A., Fungal community dynamics and driving factors during agricultural waste composting, Environ. Sci. Pollut. Res., 22 (2015), pp. 19879–19886.
Yu, J., Deem, L.M., Crow, S.E., Deenik, J.L., Penton, C.R., 2018. Biochar application influences microbial assemblage complexity and composition due to soil and bioenergy crop type interactions. Soil Biol. Biochem. 117, 97–107.
Yuan, D.X., 1997. Rock desertification in the subtropical karst of South China. Z. Geomorphol. 108, 81–90.
Zhang, Y., Tan, Q., Hu, C., Zheng, C., Gui, H., Zeng, W., Sun, X., Zhao, X., 2015. Differences in responses of soil microbial properties and trifoliate orange seedling to biochar derived from three feedstocks. J. Soils Sediments 15, 541–551.
Zhang, C., Liu, G., Xue, S., Wang, G., 2016. Soil bacterial community dynamics reflect changes in plant community and soil properties during the secondary succession of abandoned farmland in the Loess Plateau. Soil Biol. Biochem. 97, 40–49.
Zhao, S., Li, K., Zhou, W., Qiu, S., Huang, S., He, P., 2016. Changes in soil microbial community, enzyme activities and organic matter fractions under long-term straw return in north-central China. Agric. Ecosyst. Environ. 216, 82–88.
Zhou, J., Deng, Y., Luo, F., He, Z., Tu, Q., Zhi, X., 2010. Functional molecular ecological networks. mBio 1.
Zhou, J., Deng, Y., Luo, F., He, Z., Yang, Y., Phylogenetic molecular ecological network of soil microbial communities in response to elevated CO2, mBio, 2 (2011).
Zhou, Z., Gao, T., Zhu, Q., Yan, T., Li, D., Xue, J., Wu, Y., 2019. Increases in bacterial community network complexity induced by biochar-based fertilizer amendments to karst calcareous soil. Geoderma 337, 691–700.